RSC Advances

ROYAL SOCIETY OF CHEMISTRY

www.rsc.org/advances

Fabrication of chitosan/silica nanofibrous adsorbent functionalized with amine groups for the removal of Ni (II), Cu (II) and Pb (II) from aqueous solutions: Batch and column studies

Vahid Sabourian[1], Ali Ebrahimi[2], Farzad Naseri[3], Mohammad Irani[4,*], Arash Rahimi[5]

[1]South pars gas production platform, Bushehr, Iran

[2]Department of chemical engineering, Islamic Azad University, north branch, Tehran, Iran

[3]Department of civil engineering, Electronic Branch, Islamic Azad University, Tehran, Iran

[4]Department of Chemical Engineering, Amirkabir University of Technology (Tehran Polytechnic), Tehran, Iran

[5]Department of Biophysics, Faculty of Basic Science, Science and Research Branch of Islamic Azad University, Tehran, Iran

Abstract

The chitosan/tetraethylorthosilicate/aminopropyl triethoxysilane (CS/TEOS/APTES) composite nanofibrous adsorbent was prepared via electrospinning process. The performance of the prepared nanofibers was investigated for the Ni (II), Cu (II) and Pb (II) ions sorption in single and ternary systems. The prepared nanofibers were characterized using FTIR, SEM and BET analysis. The effects of sorption parameters including pH, contact time, initial concentration and temperature were evaluated in a single system. The maximum sorption capacities of Ni (II), Cu (II) and Pb (II) ions onto the CS/TEOS/APTES nanofibrous adsorbent were found to be 696.2, 640.5 and 575.5 mg g^{-1} at equilibrium time of 30 min and 45 ˚C. The kinetic and equilibrium data were well described by pseudo-first-order kinetic and Langmuir isotherm models. The

* Corresponding author. Tel.: +98 021 22590926; fax: +98 021 22600600. E-mail address: irani_mo@ut.ac.ir (M. Irani).

calculated thermodynamic parameters indicated a spontaneous and endothermic adsorption process. The Box–Behnken design was used to evaluate the effects of four parameters including pH and initial concentrations of Ni (II), Cu (II) and Pb (II) ions on the sorption efficiency. The selectivity order of metal ions onto the CS/TEOS/APTES nanofibers was Ni (II)>Cu (II)>Pb (II) in a ternary system. In fixed bed column studies, the Ni (II), Cu (II) and Pb (II) sorption capacities were increased by increasing the flow rate up to 4 mL min^{-1}. Thomas model was well predicted the adsorption capacity of metal ions in a fixed bed column. The removal efficiency of metal ions by the regenerated nanofibers, did not significantly change in both batch and fixed-bed column studies.

Key words: Chitosan/TEOS/APTES, Nanofibers, Heavy Metal, Ternary System, Column Studies

1. Introduction

Removal of heavy metal ions from water and wastewater is of primary importance with respect to human's health and environmental considerations. Several methods including chemical precipitation, membrane filtration, solvent extraction and adsorption have been used for the removal of heavy metal ions from aqueous solutions [1]. The adsorption process due to the low cost and higher efficiency is commonly preferred [2, 3]. The nanofibers prepared by electrospinning process due to the unique properties including high specific surface area and high porosity with fine pores have been widely applied for adsorption process [4]. In recent studies, the nanofibrous adsorbents based on both synthetic and natural polymers such as polyvinyl alcohol (PVA) [5-7], polyvinylpyrrolidone (PVP) [8], polyacrylonitrile (PAN) [9, 10], cellulose [11] and chitosan [12-16] were used for the removal of heavy metal ions. Chitosan nanofibers due to the higher surface area and ion exchange properties have been used as an alternative

adsorbent for metal ions sorption [14, 15]. The presence of hydroxyl and amino groups in the chitosan network allow the uptake of heavy metal ions during chelation, electrostatic attraction or ion-exchange mechanisms. Furthermore, the chemical modification of chitosan nanofibers improves the removing efficiency of metal ions [16, 17]. The functional groups such as Si-H, Si-OH and N-H groups in the tetraethylorthosilicate (TEOS), as the silica precursor [6, 18], and aminopropyl triethoxysilane (APTES), as an aminated silica precursor [6], have significant effect in improving adsorption efficiency. However, there is no study about incorporation of TEOS and APTES into the chitosan nanofibers and investigation of sorption behavior.

To investigate the simultaneous removal of metal ions onto the adsorbent, the statistical design of experiments was applied to reduce the number of experiments and consider the interactions in multivariable systems [19, 20]. Response surface methodology (RSM) is essentially a particular set of mathematical and statistical methods for developing, improving and optimizing the processes. Recently, RSM was used for the optimization of the process conditions in the removal of heavy metal ions from aqueous solutions [21-23]. The RSM based on Central-Composite Design (CCD) and Box–Behnken Design (BBD) are commonly used as experimental design techniques [19, 20]. However, for a quadratic response surface model with three or more factors, the BBD technique is much more advantageous compared with CCD [20].

In the present study, the CS/TEOS/APTES nanofibrous adsorbent was prepared via electrospinning process and its application for the removal of Ni (II), Cu (II) and Pb (II) ions from aqueous solutions was investigated in a batch and fixed bed column systems. The influence of pH, contact time, initial concentration and temperature on the adsorption process was evaluated in a single system. The nature of the adsorption process with respect to its kinetics, isotherms and thermodynamic aspects was determined. The reusability of CS/TEOS/APTES was

tested after five adsorption–desorption cycles. After optimization of parameters for maximum adsorption capacities of metal ions, RSM based on BBD was used to evaluate the interaction effects of pH, and initial concentrations of Ni (II), Cu (II) and Pb (II) ions on the simultaneous adsorption of metal ions in ternary system. The experimental data from fixed bed column system were also fitted to the Thomas model. Desorption studies were carried out in both batch and fixed bed column systems.

2. Experimental

2.1 Materials

Chitosan (average Mw = 200 kD), TEOS (density = 940 kg m^{-3}), APTES (99%), cetyltrimethylammonium bromide (CTAB), ethanol and HCl were purchased from Sigma–Aldrich. Deionized water was used throughout this work.

2.2 Preparation of CS/TEOS/APTES solution

The chitosan solution was prepared by dissolving chitosan in 0.5 M acetic acid under magnetic stirring condition for 24 h at 30 ˚C. Then, TEOS and APTES were added to the chitosan solution.

The TEOS mixture was prepared by mixing CTAB:TEOS: HCl:H_2O:ethanol in the molar ratio of 1:4:0.1:200:50. For this, CTAB was mixed with water and ethanol for 10 min at 30 ˚C. Then, 20 wt% TEOS was added to the solution with stirring for further 1 h. After that, HCl was dropped slowly into the solution to prepare the TEOS mixture. Then, 0.5 mL of APTES was added to the TEOS mixture and the stirring was continued at for further 1 h. Finally, the TEOS/APTES mixture was added to the chitosan solution with stirring for further 6 h at 30 ˚C.

2.3 Electrospinning process

In order to fabrication of CS/ TEOS/APTES nanofibers, the CS/ TEOS/APTES solution was loaded into the 5 mL plastic syringe equipped with a syringe needle. After that, a high voltage was applied between the needle and the collector and CS/ TEOS/APTES nanofibers were produced on the collector. A voltage of 25 kV, with a tip-collector distance of 12 cm, at a speed of 0.2 mL h^{-1} was applied to fabricate the nanofibers on the cylindrical collector. Then, 25% glutaraldehyde (GTA) vapor was used for cross-linking of CS/ TEOS/APTES nanofibers. Finally, the nanofibers were dried at 30˚C for 24 h.

2.4 Characterization

The functional groups of nanofibers were determined by Fourier transform infrared spectroscopy (Vector22-Bruker Company, Germany) in the range of 400–4000 cm^{-1}.

The morphology of the nanofibers was determined using a scanning electron microscopy (SEM, JEOL JSM-6380) after gold coating. The average diameter and diameter distribution of nanofibers were obtained with an image analyzer (Image-Proplus, Media Cybrernetics). From each image, at least 50 different fiber segments were randomly selected and their diameters were measured to generate an average fiber diameter.

The average pore diameter, specific surface area and pore volume of the prepared nanofibrous adsorbents were measured with nitrogen adsorption and Brunauer–Emmett–Teller (BET) method on a Quantachrome Autosorb-1 instrument.

The final concentration of heavy metal ions in the adsorption medium was determined using an inductively coupled plasma atomic emission spectrophotometer (ICP-AES, Thermo Jarrel Ash, Model Trace Scan).

2.5 Adsorption experiments in a single system

The metal ions sorption onto the CS/ TEOS/APTES nanofibers were carried out as functions of pH (2-7), contact time (0-60 min), initial concentration (20-1000 mg L^{-1}) and temperature (25-45 ˚C) in a batch system. The sorption experiments were carried out in 250 mL flasks containing 50 mg of the adsorbent in 100 mL of metal ions solutions (100 mg L^{-1}) on a rotary shaker at 200 rpm for 1 h at the different pH levels. For determining the effect of contact time on metal ions sorption, experiments were done by placing 50 mg of adsorbent in 100 mL of metal solutions (100 mg L^{-1}) at 25 ˚C and the optimum pH at definite time intervals. For examining the effect of initial concentration of metal ions and temperature, 50 mg of the nanofibrous samples was rinsed in 100 mL of metal ions solutions with concentrations varying in the range of 20–1000 mg L^{-1} at three different temperatures (25, 35 and 45 ˚C) for 1 h.

For regeneration of nanofibrous adsorbents, the nanofibers were rapidly washed with 1 M HNO_3 for 1 h and then were washed several times with deionized water. Desorption experiments were carried out with the initial metal concentration of 100 mg L^{-1}, adsorbent dosage of 0.5 g L^{-1}, optimum pH, contact time of 1 h temperature of 25 ˚C.

. After that, the nanofibers were dried in an oven at 60 ˚C for 1 h. Each experiment was repeated triplicate and the results were given as an average. The adsorption capacity (q_e (mg g^{-1})) and removal percentage (R (%)) are calculated as follows:

$$q_e = \frac{(C_0 - C_e)\,V}{1000M} \qquad (1)$$

$$R(\%) = \frac{(C_0 - C_e)}{C_0} \times 100 \qquad (2)$$

where C_0 and C_e are the initial and equilibrium concentrations of metal ions solution in mg L^{-1}, V is the volume of the solution in mL and M is the weight of the adsorbent in g.

2.6 Design of experiments in a ternary system

Box-Behnken design (BBD) is a class of rotatable second-order designs based on three level incomplete factorial designs where the variable combinations are at the midpoints of the edges of the variable space and at the center. The number of experiments (N) needed for the development of BBD is defined as $N = 2k(k - 1) + C_0$, where (k) is the factor number and (C_0) is the replicate number of the central point. In the current study, four factors three levels BBD was used to determine the relation between variables containing pH (5–6), and Ni (II), Cu (II) and Pb (II) initial concentrations (20–100 mg/L) on the removal of metal ions in a ternary system. Contact time of 30 min and temperature of 45 ˚C were considered constants in the experiments. The polynomial models for the metal ions removal percentage were expressed as follows:

$$Y = \beta_0 + \sum_{i=1}^{4} \beta_i X_i + \sum_{i=1}^{4} \beta_{ii} X_i^2 + \sum_{i=1}^{4} \sum_{j=1}^{4} \beta_{ij} X_i X_j \qquad (3)$$

where Y is the predict response by the model and β_0, β_i, β_{ii}, β_{ij} are the constant regression coefficients of the model. X_i, X_{ii} and X_{ij} represent the linear, quadratic and interactive terms of the uncoded independent variables, respectively. The coefficient of determination (R^2) was used to evaluate the accuracy of the full quadratic equation. The experimental design and results of metal ions removal percentages onto the CS/ TEOS/APTES nanofibrous adsorbent are presented in Table 1.

Table 1 Experimental design and results of metal ions sorption onto the CS/ TEOS/APTES nanofibers

Run number	pH (X_1)	Ni (II) initial concentration (mg/L) (X_2)	Cu (II) initial concentration (mg/L) (X_3)	Pb (II) initial concentration (mg/L) (X_4)	Ni (II) removal (%)	Fitted value (%)	Cu (II) removal (%)	Fitted value (%)	Pb (II) removal (II)	Fitted value (%)
1	5.0	20	60	60	93±2	91	55±2	56	50±1	50
2	6.0	20	60	60	83±3	87	59±1	59	52±2	52
3	5.0	100	60	60	61±1	63	42±2	43	37±2	38
4	6.0	100	60	60	60±2	60	48±1	48	39±2	40
5	5.5	60	20	20	68±3	66	87±2	86	82±1	82
6	5.5	60	100	20	65±2	65	37±2	36	68±2	68
7	5.5	60	20	100	66±1	66	77±1	78	32±2	33
8	5.5	60	100	100	50±2	51	30±3	32	25±2	26
9	5.0	60	60	20	66±2	67	51±2	53	69±1	68
10	6.0	60	60	20	65±1	64	55±2	58	71±1	70
11	5.0	60	60	100	59±2	60	47±3	48	24±1	23

12	6.0	60	60	100	56±1	57	50±2	51	26±1	25
13	5.5	20	20	60	94±2	93	86±2	87	62±2	61
14	5.5	100	20	60	62±3	65	72±3	74	52±1	51
15	5.5	20	100	60	85±2	85	37±2	38	53±2	52
16	5.5	100	100	60	59±2	57	26±1	28	39±1	38
17	5.0	60	20	60	68±2	68	81±2	79	50±2	51
18	6.0	60	20	60	66±3	64	84±3	82	52±1	53
19	5.0	60	100	60	58±2	60	32±2	30	40±1	40
20	6.0	60	100	60	56±1	56	37±1	35	42±1	42
21	5.5	20	60	20	92±2	92	60±2	59	81±2	82
22	5.5	100	60	20	60±3	64	55±2	53	65±1	65
23	5.5	20	60	100	86±3	85	60±3	58	30±2	31
24	5.5	100	60	100	60±2	58	45±3	42	26±1	25
25	5.5	60	60	60	64±2	62	60±1	60	50±2	50
26	5.5	60	60	60	64±2	62	59±2	60	49±3	50
27	5.5	60	60	60	63±3	62	60±1	60	50±2	50

2.7 Adsorption experiments in fixed bed column

Fixed bed adsorption used in this study was performed in a glass column with height of 100mm and internal diameter of 15mm, each filled with known quantity (1g) of the CS/ TEOS/APTES nanofibrous adsorbent. The initial concentration of metal ions was held constant at 50 mg/L and the input flow rate was 1, 2, 4 and 6 mL min^{-1} that was controlled by a peristaltic pump. In order to investigate the desorption process, an experiment was carried out by desorbing the previously adsorbed metal ions by passing 1 M HNO_3 through the bed column containing nanofibers.

3 Results and discussion

3.1 Characterization of CS/ TEOS/APTES nanofibers

The functional groups of CS and CS/TEOS/APTES nanofibers were characterized using Fourier Transform Infrared (FTIR). The results are shown in Fig.1. The broad band in the 3200-3600 was assigned to the O−H and N−H groups in the chitosan chain. The bands at 1650 and 1560 cm^{-1} correspond to the amino I and amino II functional groups of chitosan. The bands in the 1020–1100 cm^{-1} was due to the presence of Si-O-Si and Si-O-C in the network of CS/TEOS/APTES nanofibers. The peak at 780 cm^{-1} was assigned to the Si-C band in the CS/TEOS/APTES

structure. The N-H stretching peak was observed at 1580 cm^{-1} which indicated that the APTES have been successfully added into the CS/TEOS/APTES structure.

The SEM images of pure CS and CS/TEOS/APTES nanofibers are shown in Fig.2. As shown, the homogeneous fibers with average diameter of 90 nm were formed for pure CS. While the increase in fibers diameter was observed for CS/TEOS/APTES nanofibers with average diameter of 138 nm. It could be attributed to the increase in viscosity of solution resulted in formation of the thicker fibers compared with pure CS nanofibers. EDAX analysis of chitosan (Fig.3c) and CS/TEOS/APTES nanofibers (Fig.3d) revealed the presence of silica and mercapto groups in the CS/TEOS/APTES structure.

The S_{BET}, pore volume and average pore diameter of pure CS and CS/TEOS/APTES nanofibers were determined using Brunauer–Emmett–Teller (BET) method. The results are shown in Table 2. Increasing of Si and N atoms of TEOS/APTES groups onto the CS nanofibers caused to decrease the adsorption of nitrogen molecules and resulted in decrease in S_{BET}, pore volume and average pore diameter of CS/TEOS/APTES nanofibers compared with pure CS nanofibers. Similar trends were reported by other researchers [25, 26]. They found that the adding Si and N atoms into the polymeric nanofibers led to decrease in S_{BET}, pore volume and pore diameter of nanofibers.

Table 2 Physical properties of prepared nanofibers

Sample	S_{BET} (m^2g^{-1})	Pore volume (cm^3 g^{-1})	Average diameter (nm)
CS	310.2	0.482	3.98
CS/TEOS/APTES	272.3	0.431	3.52

Fig.1********

********Fig.2**********

*********Table 2 *********

3.2 Batch adsorption experiments in a single mode

The effect of pH on the Ni (II), Cu (II) and Pb (II) ions sorption using pure CS and CS/TEOS/APTES nanofibers is shown in Fig.3. As shown the adsorption capacities of metal ions onto the CS and CS/TEOS/APTES nanofibrous adsorbents reached the maximum values at pH values of 5, 6 and 5.5 for Ni (II), Cu (II) and Pb (II) ions sorption, respectively. At lower pH values, the competition of hydrogen ion with metal ions in chelating with anion functional groups of nanofibrous adsorbents led to decrease the adsorption capacities of metal ions onto the both CS and CS/TEOS/APTES nanofibers. At pH above optimum pH values, the formation of hydroxylated complexes of metal ions in the forms of $Ni(OH)_2$, $Cu(OH)_2$ and $Pb(OH)_2$ resulted in decrease in adsorption capacities of metal ions onto the CS and CS/TEOS/APTES nanofibers [18, 24, 25]. Furthermore, the metal ions sorption using CS/TEOS/APTES nanofibrous adsorbent was higher than that of CS nanofibers. This behavior could be attributed to the incorporation of negative functional groups including siloxane, silanol and amine groups into the chitosan network which enhanced the available active sites for adsorption process. Also, the results showed that the adsorption capacity of different metal ions increased in order of Pb(II)< Cu(II)<Ni(II). The ionic radius range for these ions are in order of Ni(II)<Cu(II)< <Pb(II). As ionic radius increases due to charge density decreases, the availability of active sites of nanofibers for adsorption process decreases; which resulted in decreasing the adsorption capacity of different metal ions by increasing the ionic radius [15]. Therefore, the pH values of 5, 6 and 5.5 were selected as optimum values of Ni (II), Cu (II) and Pb (II) ions sorption onto the CS/TEOS/APTES nanofibrous adsorbent for further experiments.

**********Fig.3**********

The effect of contact time on the adsorption of Ni (II), Cu (II) and Pb (II) ions onto the CS/TEOS/APTES nanofibers is shown in Fig.4. As shown, the metal ions sorption onto the nanofibrous adsorbent reached the equilibrium after only 30 min. Therefore, 30 min is selected as equilibrium time for further experiments. The pseudo-first-order and pseudo-second-order kinetic models were used to describe the kinetic data of metal ions using CS/TEOS/APTES nanofibrous adsorbent. The kinetic equations are expressed as follows [27, 28]:

Pseudo-first-order $$q_t = q_e(1-\exp(-k_1 t)) \quad (4)$$

Pseudo-second-order $$q_t = \frac{k_2 q_e^2 t}{1+k_2 q_e t} \quad (5)$$

where q_t and q_e (mg g^{-1}) are the adsorption capacities of metal ions at time t and equilibrium time, respectively. k_1 (min^{-1}) and k_2 (g $mg^{-1}min^{-1}$) are the pseudo-first-order and pseudo-second-order rate constants, respectively. The results are presented in Table 3. The results showed that pseudo-first-order kinetic model (R^2>0.994) was well described the kinetic data of metal ions onto the CS/TEOS/APTES nanofibrous adsorbent.

**********Fig.4**********

*******Table 3 **********

Table 3: Kinetic parameters of metal sorption onto the CS/TEOS/APTES nanofibrous adsorbent

Metal ion	Pseudo-first-order model			Pseudo-second-order model		
	q_{eq} (mg/g)	K_1 (min^{-1})	R^2	q_{eq}	K_2 (g/mg.min)	R^2
Ni^{2+}	190.1	0.1025	0.994	223.0	0.000569	0.990
Cu^{2+}	177.9	0.1032	0.994	208.5	0.000615	0.989
Pb^{2+}	158.0	0.1039	0.995	185.0	0.000699	0.989

The effect of initial concentration of metal ions on the adsorption capacity of nanofibers at three different temperatures (25, 35 and 45 ˚C) is shown in Fig. 5. As shown, the metal ions sorption capacity was increased by increasing the temperature which indicated that the adsorption process onto the CS/TEOS/APTES nanofibrous adsorbent was favorable at higher temperatures. The known Freundlich and Langmuir isotherm models were used to describe the equilibrium data of metal ions sorption using CS/TEOS/APTES nanofibers.

**********Fig.5**********

The isotherm equations are expressed as follows [29-31]:

Freundlich isotherm model $$q_e = k_F C_e^{\frac{1}{n}} \quad (6)$$

Langmuir isotherm model $$q_e = q_m \frac{bC_e}{1+bC_e} \quad (7)$$

where k_F (mg g^{-1}) and n are Freundlich parameters related to the sorption capacity and intensity of the sorbent, respectively. q_m (mg g^{-1}) and b (mg^{-1}) are the Langmuir model constants. q_m is the maximum value of metal ion adsorption per unit weight of adsorbent that is related to the monolayer adsorption capacity and b is related to the enthalpy of adsorption. The parameters of isotherm models were calculated by nonlinear regression of q_e versus C_e using MATLAB software. The results are shown in Table 4. By comparing the correlation coefficients, it was found that the equilibrium data was best described by Langmuir isotherm model ($R^2 > 0.984$) compared with Freundlich ($R^2 > 0.911$) isotherm model. This behavior indicated the monolayer reaction of metal ions using CS/TEOS/APTES nanofibers. Furthermore, the adsorption of metal ions increased slightly as the temperature increased from 25 to 45 ˚C at higher concentrations of Ni (II), Cu (II) and Pb (II) ions. This indicates that a high temperature favored the adsorption

process using CS/TEOS/APTES nanofibrous adsorbent at higher initial concentrations of metal ions.

********Table 4**********

Table 4 Isotherm parameters for metal adsorption onto the CS/TEOS/APTES nanofibrous adsorbent

Metal	T(ºC)	Freundlich isotherm			Langmuir isotherm		
		K_F (mg/g)	n	R^2	q_{max} (mg/g)	K_L (L/mg)	R^2
Ni^{2+}	25	148.3	4.081	0.901	662.0	0.06451	0.998
	35	167.2	4.273	0.909	684.9	0.08157	0.998
	45	189.4	4.566	0.911	696.2	0.11420	0.997
Cu^{2+}	25	111.2	3.564	0.888	619.3	0.03870	0.997
	35	123.8	3.817	0.892	630.0	0.04721	0.998
	45	145.4	4.150	0.884	640.5	0.06173	0.992
Pb^{2+}	25	72.4	3.191	0.929	553.7	0.01964	0.995
	35	77.8	3.248	0.940	570.0	0.02041	0.994
	45	88.9	3.441	0.941	575.5	0.02356	0.990

The thermodynamic parameters including Gibbs free energy change (ΔG°), entropy change (ΔS°) and enthalpy change (ΔH°) for metal ions sorption using CS/TEOS/APTES nanofibrous adsorbents were evaluated by the following equations:

$$k_C = \lim_{C_{el} \to 0} \frac{C_{es}}{C_{el}} \qquad (8)$$

$$\Delta G^0 = -RT \ln k_C \qquad (9)$$

$$\ln k_C = \frac{\Delta S^0}{R} - \frac{\Delta H^0}{RT} \qquad (10)$$

where R (kJ $mol^{-1}K^{-1}$) is the gas constant, and T (K) is the temperature. C_{es} and C_{el} are the values of solid and liquid phase concentration in equilibrium (mg L^{-1}) respectively. The thermodynamic

parameters are summarized in Table 5. The negative values of ΔG° showed the spontaneous nature of the metal sorption using CS/TEOS/APTES nanofibrous adsorbent. The positive values of ΔH° indicated the endothermic nature of metal ions sorption using nanofibrous adsorbent. The positive values of ΔS° showed that the randomness was increased at the solid-solution interface.

**********Table 5 **********

Table 5 Thermodynamic parameters for metal adsorption onto the CS/TEOS/APTES nanofibrous adsorbent

Metal	K_C			ΔH° (kJ/mol)	ΔS° ($kJ/mol.K$)	ΔG° (kJ/mol)		
	25ºC	35ºC	45ºC			25ºC	35ºC	45º
Ni^{2+}	73.07	121.57	156.21	30.03	0.1370	-10.632	-12.293	-13.355
Cu^{2+}	19.10	29.65	42.88	31.89	0.1315	-7.308	-8.680	-9.937
Pb^{2+}	11.66	19.33	31.89	39.62	0.1533	-6.0853	-7.584	-9.154

The result of five cycles of adsorption/desorption of metal ions onto CS/TEOS/APTES nanofibrous adsorbent is shown in Fig.6. Result showed that the sorption capacities of metal ions using CS/TEOS/APTES nanofibrous adsorbent were slightly decreased after five adsorption/desorption cycles. The reduction in the adsorption capacity of the nanofibers for metal ions sorption could be attributed to the physically losing some functional groups of CS/TEOS/APTES nanofibrous adsorbent (such as Si-H, Si-OH and N-H) by the acid cleavage. The maximum sorption capacities of metal ions onto the CS/TEOS/APTES nanofibrous adsorbent were compared with that of the other nanofibrous adsorbents which results are presented in Table 6. As shown, the sorption capacities of metal ions onto the CS/TEOS/APTES nanofibers were found to be comparable and moderately higher than those of many corresponding sorbents in the literature [10, 11, 14-17, 32-34]. The higher surface area and more

functional groups of prepared nanofibers including Si-H, Si-OH and N-H groups in the CS/TEOS/APTES structure may be responsible for higher sorption of metal ions using CS/TEOS/APTES nanofibrous adsorbent.

**********Fig.6 **********

*********Table 6 **********

Table 6 Comparison of adsorption capacity (mg g^{-1}) of synthesized CS/TEOS/APTES nanofibers for metal ions sorption with other nanofibrous adsorbents reported in the literature

Adsorbent	Adsorption capacity of Ni (II) (mg g^{-1})	Adsorption capacity of Cu (II) (mg g^{-1})	Adsorption capacity of Pb (II) (mg g^{-1})	Reference
Amidoxime-PAN	---	52.70	263.45	[10]
Aminated-PAN	---	116.20	---	[11]
Chitosan	---	485.44	263.15	[14]
PEO/Chitosan	357.10	310.20	237.20	[15]
Chitosan/ hydroxyapatite	180.20	---	296.70	[16]
Lead-chitosan	---	---	577.00	[17]
PVA/ZnO	94.43	162.80	---	[31]
PAN/cellulose/Thiol	---	---	137.70	[32]
Chitin	135.00	---	302.51	[33]
CS/TEOS/APTES	715.70	715.70	579.10	This study

3.3 Batch adsorption experiments in a ternary system

Analysis of variance (ANOVA) was performed to estimate the significance of the model and terms. The P values lower than 0.05 indicating the significant of the terms on the surface response analysis. The results are presented in Table 7. As shown, the linear terms as well as some quadratic and interaction terms exhibited significant effect on the metal ions sorption efficiency using CS/TEOS/APTES nanofibers ($p<0.05$). By elimination of insignificant terms ($p>0.05$) from the full quadratic model, the equations of 11-13 for Ni(II) (R_1), Cu (II) (R_2) and Pb (II) (R_3) removal percentages (%) were obtained; as follows:

$$R_1= 62.067-1.833X_1-13.667X_2-3.917X_3-3.417X_4+12.933X_2^2-3.250X_3X_4 \quad (11)$$

$$R_2=60.741+2.083X_1-5.750X_2-24.000X_3-3.000X_4-4.819X_1^2-4.319X_2^2-3.194X_4^2-2.500X_2X_4 \quad (12)$$

$R_3=49.481+1.000X_1-5.833X_2-5.250X_3-22.750X_4-4.389X_1^2+1.236X_3^2+1.486X_4^2+3.000X_2X_4+1.750\ X_3X_4$ (13)

The high values of R^2 ($R_1^2>0.97$, $R_2^2>0.96$ and $R_3^2>0.99$ for Ni(II), Cu (II) and Pb (II)) indicated a high reliability of the model in predicting the removal percentages of metal ions. The probability distribution plots of residuals (difference between the model predicted and those derived experimentally) for the metal ions removing percentages (%) are shown in Fig. 7. As shown, for all of the results, the errors were normally distributed which indicated that the predicted models fitted well all the experimental data of metal ions removing percentages (%).

**********Table 7 **********

*****Fig.7**********

Table 7: ANOVA results for (a) Ni (II), (b) Cu (II) and (c) Pb (II) ions sorption onto the CS/TEOS/APTES nanofibrous adsorbent

(a)

Source	F	P
Regression	67.02	0.000
Linear	161.46	0.000
X_1	10.00	0.008
X_2	555.51	0.000
X_3	45.62	0.000
X_4	34.72	0.000
Square	69.76	0.000
X_1^2	1.11	0.313
X_2^2	201.07	0.000
X_3^2	2.21	0.163
X_4^2	0.83	0.381
Interaction	2.23	0.112
X_1X_2	0.56	0.470
X_1X_3	0.56	0.470
X_1X_4	0.25	0.628
X_2X_3	0.56	0.470
X_2X_4	0.99	0.339
X_3X_4	10.47	0.007
Lack-of-Fit	14.32	0.067
Total		

(b)

Source	F	P
Regression	90.78	0.000
Linear	307.29	0.000
X_1	8.57	0.013
X_2	65.29	0.000
X_3	1137.52	0.000
X_4	17.77	0.001
Square	9.12	0.001
X_1^2	17.12	0.001
X_2^2	13.46	0.003
X_3^2	1.28	0.280
X_4^2	6.84	0.023
Interaction	0.87	0.543
X_1X_2	0.16	0.692
X_1X_3	0.16	0.692
X_1X_4	0.04	0.843
X_2X_3	0.37	0.554
X_2X_4	4.11	0.049
X_3X_4	0.37	0.554
Lack-of-Fit	21.68	0.045
Total		

(c)

Source	F	P
Regression	371.87	0.000
Linear	1259.43	0.000
X_1	8.68	0.012
X_2	295.48	0.000
X_3	239.34	0.000
X_4	4494.21	0.000
Square	32.66	0.000
X_1^2	76.71	0.000
X_2^2	0.17	0.690
X_3^2	5.25	0.041
X_4^2	7.75	0.017
Interaction	6.30	0.003
X_1X_2	0.00	1.000
X_1X_3	0.00	1.000
X_1X_4	0.00	1.000
X_2X_3	2.89	0.115
X_2X_4	26.05	0.000
X_3X_4	8.86	0.012
Lack-of-Fit	4.77	0.185
Total		

By solving the statistical models and optimization of variables, the optimal uncoded values of pH (X_1), initial Ni (II) concentration (X_2), initial Cu (II) concentration (X_3) and initial Pb (II) concentration (X_4) were estimated to be initial concentrations of 20 mg/L at pH values of 5.0, 6.0 and 5.56 for Ni (II), Cu (II) and Pb (II) ions removing percentages, respectively. The optimum predicted values for metal ions removing percentages sorption were estimated to 94.4, 90.8 and 85.7%, respectively. The experimental values for Ni (II), Cu (II) and Pb (II) removal percentages in optimum conditions were found to be 95, 90 and 85%, respectively. These values were in good agreement with the estimated values by the model in optimum conditions.

The simultaneous relation between the metal ions initial concentrations on the adsorption capacity of metal ions is shown in Fig. 8. As shown, the effect of Ni (II) ions on the Cu (II) and Pb (II) removing percentages onto the CS/TEOS/APTES nanofibrous adsorbent was more than that of Cu (II) and Pb (II) ions effects on the Ni (II) removal percentage. Also, the sorption selectivity of Ni (II), Cu (II) and Pb (II) ions onto the CS/TEOS/APTES nanofibrous adsorbent was in order of Ni(II)> Cu(II)>Pb(II) in the ternary system. The lower ionic radius of Ni(II) ions (Ni(II)<Cu(II)< <Pb(II)) could be responsible for easier availability of Ni(II) ions for chelating with the active sites of nanofibrous adsorbent compared with Cu (II) and Pb (II) ions.

**********Fig.8**********

3.4 Adsorption experiments in a fixed bed column

The breakthrough curves of metal ions sorption using CS/TEOS/APTES nanofibrous adsorbent at different flow rates are illustrated in Fig.9. As shown, the breakthrough time decreased by enhancement in flow rate. This behavior could be attributed to insufficient residence time of the solute in the column, which caused the metal solutions to leave the column before equilibrium occurred. Also, the removal percentages of metal ions were lower in fixed bed column compared

with metal ions sorption in a batch mode. It was because of the metal ions flowing through the column did not reached equilibrium. Moreover, the metal ions sorption capacities were increased by increasing the flow rate up to 4 mL min^{-1}. The results showed that the Ni (II), Cu (II) and Pb (II) ions sorption onto the nanofibrous adsorbent could be controlled by diffusion limitations of the solute into the pores of sorbent. When the flow rate increased from 4 to 6 mL min^{-1}, the liquid residence time in the column decreased and following the sorption capacity deceased. Also, the time to reach the plateau of C_t/C_o was significantly higher for Pb (II) than Ni (II) and Cu (II).

The known Thomas model predicted the adsorption capacity of Ni (II), Cu (II) and Pb (II) ions by the CS/TEOS/APTES. Thomas model assumed that rate driving force obeys second order reversible reaction kinetics, and the adsorption equilibrium follows the Langmuir model [35]. The Thomas model is expressed as follows:

$$\frac{C_t}{C_0} = \frac{1}{1+\exp(((M \times q_0 \times k_{Th})/Q) - (C_0 \times k_{Th} \times t)/1000)} \qquad (14)$$

where C_0 (mg L^{-1}) and C_t (mg L^{-1}) are the initial concentration and final concentration at time t, respectively; M is the mass of adsorbent (g) and Q is the filtration flow rate. k_{Th} is the Thomas rate constant (l min^{-1} g^{-1}) and q_0 is the maximum uptake capacity (mg g^{-1}). The model parameters k_{Th} and q_0 can be estimated by non-linear fitting to the experimental data of breakthrough curves. The model constants (k_{Th} and q_0) and correlation coefficients are presented in Table 8 (Figure is not shown). As shown, decrease in k_{Th} and increase in q_0 was obtained by increasing the flow rate up to 4 mL min^{-1}. Based on obtained results of correlation coefficients (R^2>0.98), it was found that the Thomas model was able to describe the complete breakthrough curves. Furthermore, Thomas model predicted the adsorption capacities (Table 8) followed the same

order as the batch Langmuir adsorption capacities (Table 4) for the different metal ions using CS/TEOS/APTES nanofibers.

Table 8 Parameters obtained from the non-linear fit of breakthrough data to the Thomas model

	Q	*Thomas model*		
Metal	*(mL min^{-1})*	k_{Th} (l g^{-1}min^{-1})	q_0 (mg g^{-1})	R^2
Pb (II)	1	0.0278	453.21	0.981
	2	0.0234	490.45	0.983
	4	0.0205	504.53	0.990
	6	0.0223	518.23	0.982
Ni (II)	1	0.0218	510.11	0.990
	2	0.0204	530.75	0.992
	4	0.0196	560.11	0.986
	6	0.0205	580.39	0.980
Cu (II)	1	0.0268	500.19	0.993
	2	0.0244	518.17	0.994
	4	0.0209	540.98	0.990
	6	0.0218	555.63	0.989

Five cycles of adsorption–desorption of metal ions onto the CS/TEOS/APTES nanofibrous adsorbent were carried out in the initial Ni (II), Cu (II) and Pb (II)concentration of 60 mg L^{-1}. Desorption of metal ions by the nanofibrous adsorbent was treated with 1 M HNO_3 which results are illustrated in Fig.10. As shown, the lack of change in nanofibers efficiency for metal ions removal was observed after five adsorption–desorption cycles.

********Fig.9**********

********Fig.10***********

4 Conclusion

In the present study, the performance of CS/TEOS/APTES nanofibrous adsorbent was investigated for the removal of Ni (II), Cu (II) and Pb (II) metal ions. The pH values of 5, 6 and 5.5 exhibited the maximum sorption capacities of Ni (II), Cu (II) and Pb (II) ions onto the CS/TEOS/APTES nanofibrous adsorbent at equilibrium time of 30 min and temperature of 45 ˚C. The kinetic data of Ni (II), Cu (II) and Pb (II) ions were well fitted by pseudo-first-order kinetic model, while the equilibrium data were well described by Langmuir isotherm model. Then, 27 experiments based on BBD for four factors at three levels were used to determine the effects of pH and initial concentrations of metal ions on the removal efficiency of CS/TEOS/APTES nanofibrous adsorbent. The results showed the selectivity order of metal ions onto the CS/TEOS/APTES nanofibers was Ni (II)>Cu (II)>Pb (II) in a ternary system. The inhibitory effect was increased by increase in initial concentrations of metal ions. This study showed the CS/TEOS/APTES nanofibers as promising adsorbent with high efficiency for adsorption process. In fixed bed column studies, the efficiency increased with increasing flow rate up to 4 mL min^{-1}. The removal efficiencies of Ni (II), Cu (II) and Pb (II) ions by the regenerated CS/TEOS/APTES nanofibers, did not remarkably change in both batch and fixed-bed column systems.

References:

[1] M. Nourbakhsh, S. Illhan, H. Ozdag, Chem. Eng. J. 2002, 85, 351.

[2] M. Irani, M. Amjadi, M.A. Mousavian, Chem. Eng. J. 2011, 178, 317.

[3] A. Sari, M. Tuzen, M. Soylak, J. Hazard. Mater. 2007, 144, 41.

[4] C.S. Ki, E.H. Gang, I.C. Um, Y.H. Park, J. Memb. Sci. 2007, 302, 20.

[5] L. Roshanfekr Rad, A. Momeni, B. Farshi Ghazani, M. Irani, M. Mahmoudi, B. Noghreh, Chem. Eng. J. 2014, 256, 119.

[6] M. Irani, A.R. Keshtkar, M.A. Moosavian, Chem. Eng. J. 2012, 200–202, 192.

[7] A.R. Keshtkar, M. Irani, M.A. Moosavian, J. Radioanal. Nucl. Chem, 2013, 295, 563.

[8] M. Teng, H. Wang, F. Li, B. Zhang, J. Colloid.Interface Sci. 2011, 355,23.

[9] A. Dastbaz, A.R. Keshtkar, Appl. Surf. Sci. 2014, 293, 336.

[10] K. Saeed, S. Haider, T.J. Oh, S.Y. Park, J. Memb. Sci. 2008, 322, 400.

[11] X. He, L. Cheng, Y. Wang, J. Zhao, W. Zhang, C. Lu, Carbohyd. Polym, 2014, 111,683.

[12] A Razzaz, S Ghorban, L Hosayni, M Irani, M Aliabadi. J. Taiwan Inst. Chem. Eng. 2016, 58, 333.

[13] H Beheshti, M Irani, L Hosseini, A Rahimi, M Aliabadi. Chem Eng J. 2016, 284, 557.

[14] H.H Najafabadi, M Irani, LR Rad, AH Haratameh, I Haririan. RSC Adv. 2015, 5,16532.

[15] M Aliabadi, M Irani, J Ismaeili, H Piri, M.J. Parnian. Chem Eng J. 2013, 220, 237.

[16] M. Aliabadi, M. Irani, J. Ismaeili, S. Najafzadeh, J. Taiwan Inst. Chem. Eng. 2014, 45,518.

[17] Y. Li, T. Qiu, X. Xu, Europ. Polym. J, 2013, 49, 1487.

[18] M. Irani, A.R. Keshtkar, M.A. Mousavian, Chem. Eng. J. 2011, 175, 251.

[19] R.H Myers, D.C Montgomery, C.M Anderson-Cook. Response surface methodology: process and product optimization using designed experiments. New York (NY): Wiley; 2009.

[20] MD Mobarake, P Jafari, M Irani. Micropor Mesopor Mater 2016, doi:10.1016/j.micromeso. 2016.02.022.

[21] Y. Zheng, A. Wang, Chem.Eng. J 2010, 162, 186.

[22] J. Landaburu-Aguirre, E. Pongrácz, P. Perämäki, R. L. Keiski, J. Hazard. Mater. 2010, 180 524.

[23] F. Gönena, Z. Aksu, J. Hazard. Mater. 2009, 172, 1512.

[24] A.R. Keshtkar, M. Irani, M.A. Moosavian. J Taiwan Inst Chem Eng 2013, 44, 279.

[25] X Xue, F Li. Micropor Mesopor Mater 2008, 116, 116.

[26] M. Irani, A. R. Keshtkar, M. A. Mousavian, Korean J. Chem. Eng. 2012, 29,1459.

[27] S. Lagergren, Handlingar, 1898, 24, 1.

[28] Y.S. Ho, G. McKay, Process Biochem. 1999, 34, 451.

[29] H.M.F. Freundlich, J. Am. Chem. Soc. 1906, 57, 385.

[30] I. Langmuir, J. Am. Chem. Soc. 1916, 38, 2221.

[31] O. Redlich, D.I. Peterson, J. Phys. Chem. 1959, 63, 1024.

[32] H. Hallaji, A.R. Keshtkar, M. A. Moosavian, J. Taiwan Inst. Chem.Eng. 2015, 46, 109.

[33] R.Yang, K.B. Aubrecht, H. Ma, R. Wang, R.B. Grubbs, B.S. Hsiao, B. Chu, Polymer, 2014, 55, 1167.

[34] D. Liu, Y. Zhu, Z. Li, D. Tian, L. Chen, P. Chen, Carbohyd. Polym, 2013, 98, 483.

[35] H.C. Thomas, Ann. N.Y. Acad. Sci. 1948, 49, 161.

Figure captions:

Fig.1 FTIR spectra of pure chitosan and CS/TEOS/APTES nanofibrous adsorbent.

Fig.2 SEM images of (a) chitosan, (b) CS/TEOS/APTES nanofibrous adsorbent, and EDAX analysis of (c) chitosan and (d) CS/TEOS/APTES nanofibers.

Fig.3 Effect of pH on the removal of metal ions sorption using chitosan and CS/TEOS/APTES nanofibrous adsorbents.

Fig.4 Effect of contact time on the removal metal ions sorption using CS/TEOS/APTES nanofibrous adsorbent.

Fig.5 Effect of initial concentration of metal ions on the removal of Ni (II), Cu (II) and Pb (II) onto the CS/TEOS/APTES nanofibrous adsorbent.

Fig.6 Five cycles of metal ions adsorption–desorption using CS/TEOS/APTES nanofibrous adsorbent.

Fig.7 Probability distribution plot of residuals for (a) Ni (II), (b) and (b) Cu (II) and Pb (II) sorption onto the CS/TEOS/APTES nanofibrous adsorbent.

Fig.8 Surface plots of simultaneous effect of initial concentrations on the sorption efficiency of (a), (b), (c) Ni (II); (d), (e), (f) Cu (II) and (g), (h), (i) Pb (II) ions onto the CS/TEOS/APTES nanofibrous adsorbent.

Fig.9 Breakthrough curves of (a) Ni (II), (b) Cu (II) and (c) Pb (II) ions sorption onto the CS/TEOS/APTES nanofibers.

Fig.10 Five cycles of adsorption–desorption of Ni (II), Cu (II) and Pb (II) ions onto nanofibrous adsorbent in fixed bed column system.

Fig.1

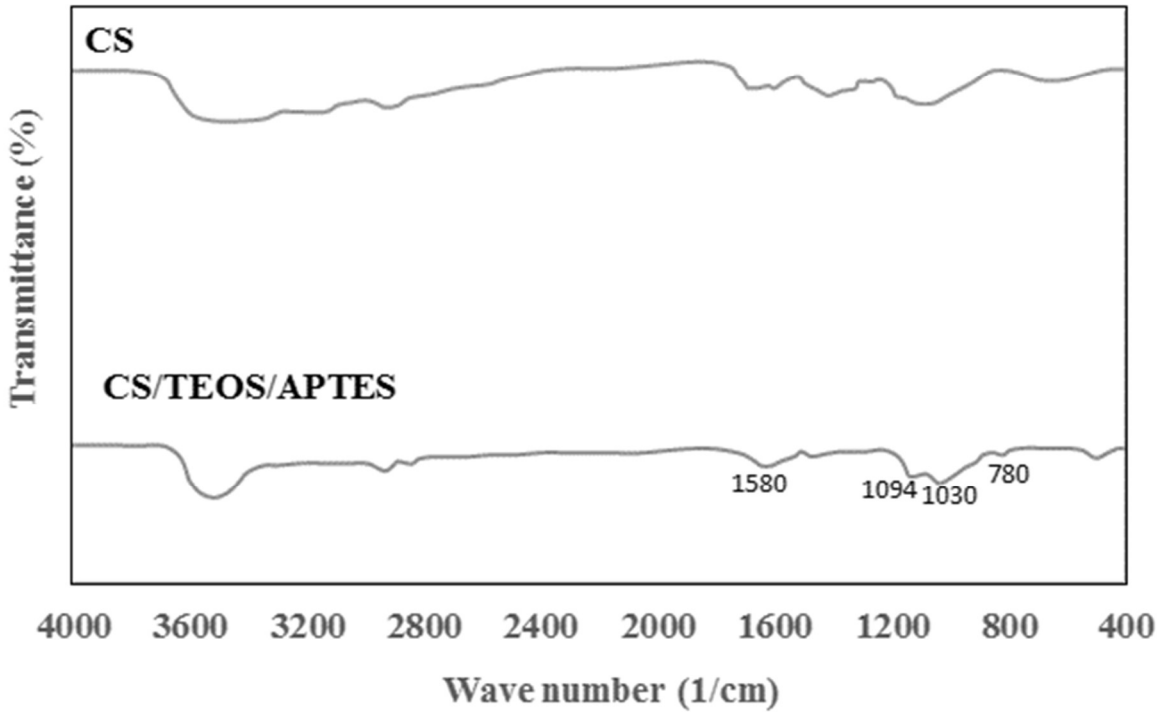

Fig.2

(a)

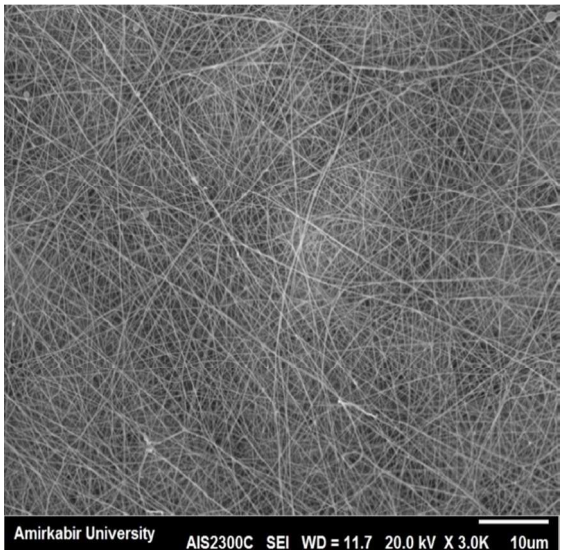

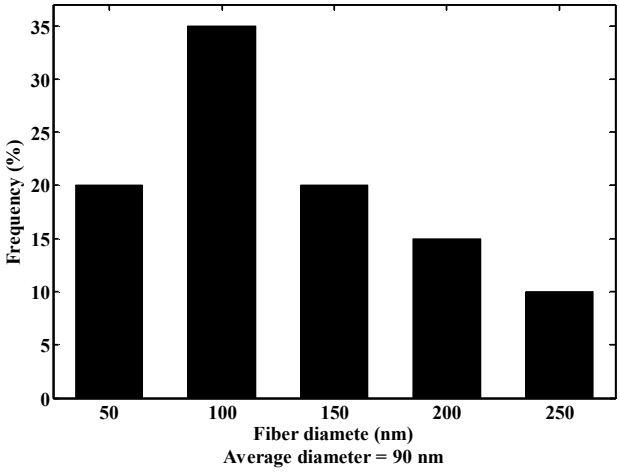

(b)

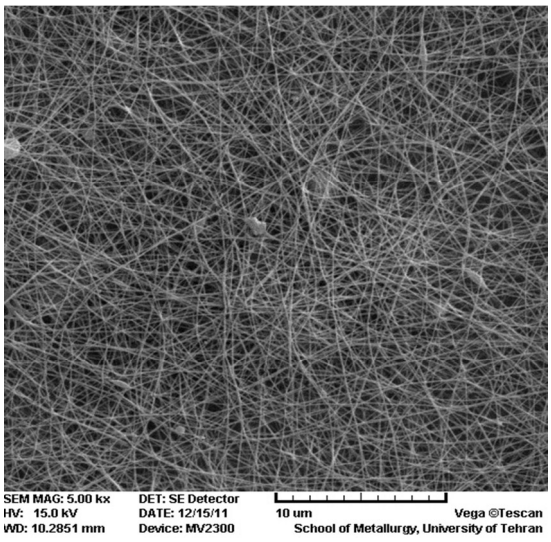

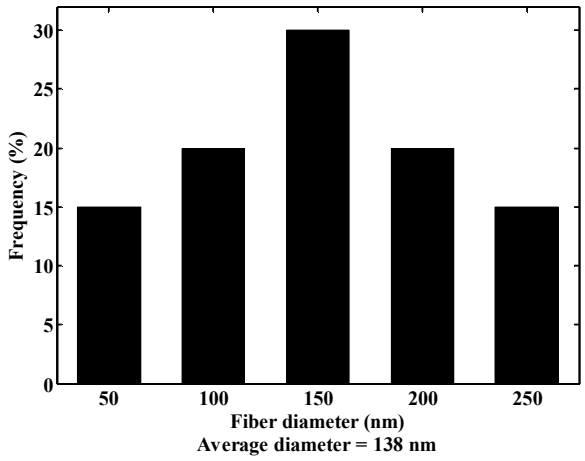

(c)

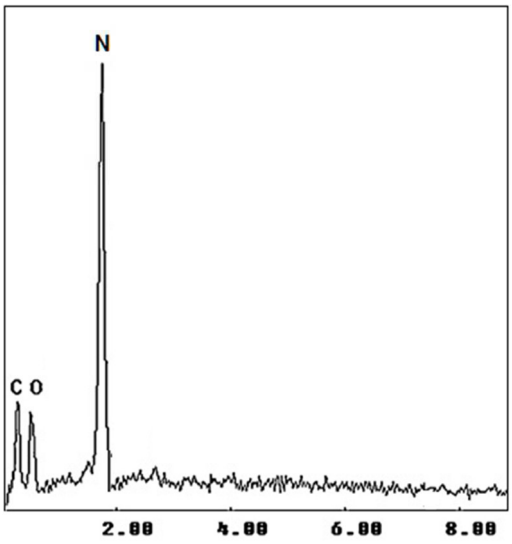

(d)

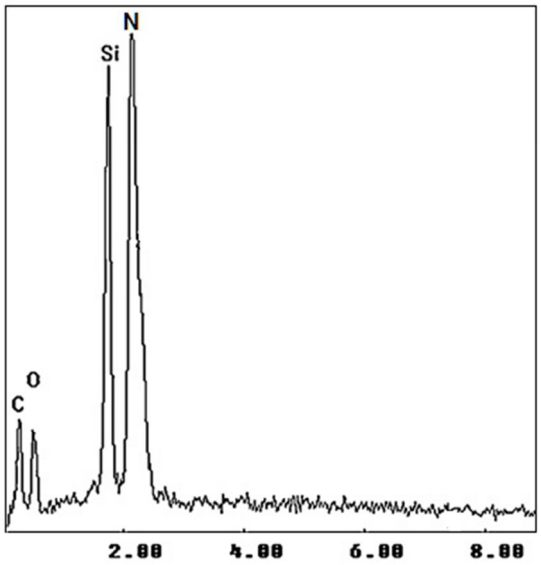

Fig.3

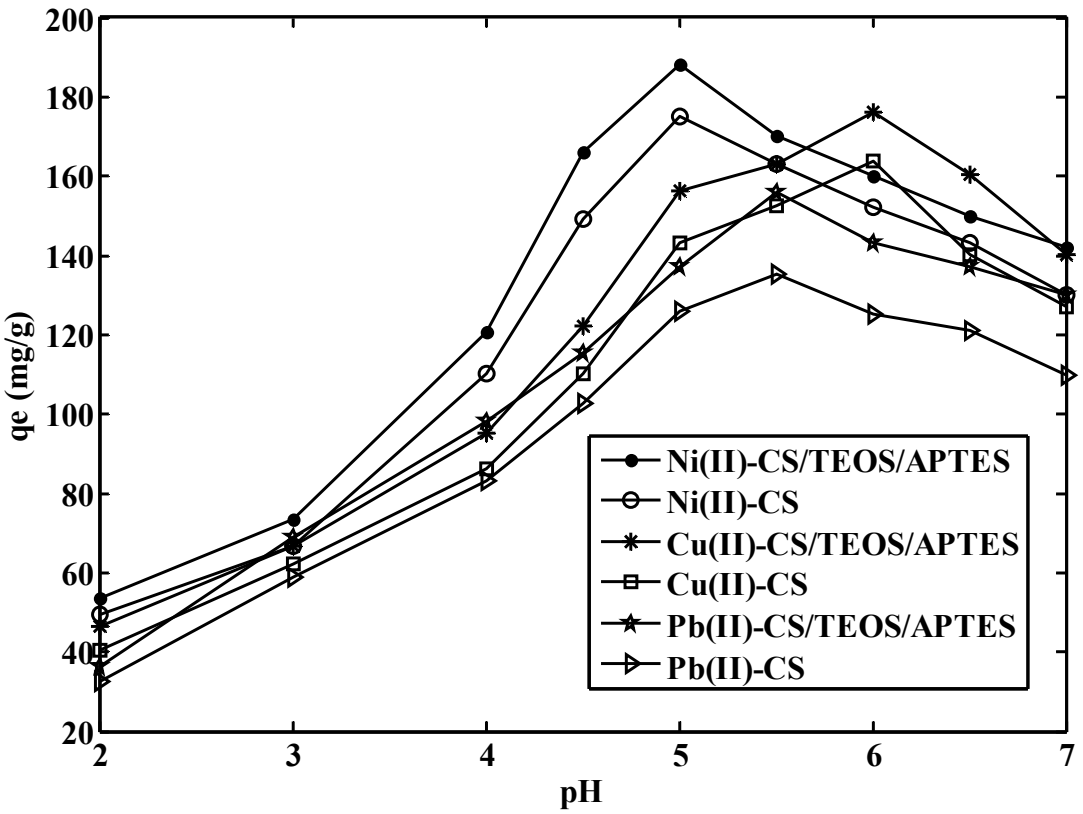

Fig.4

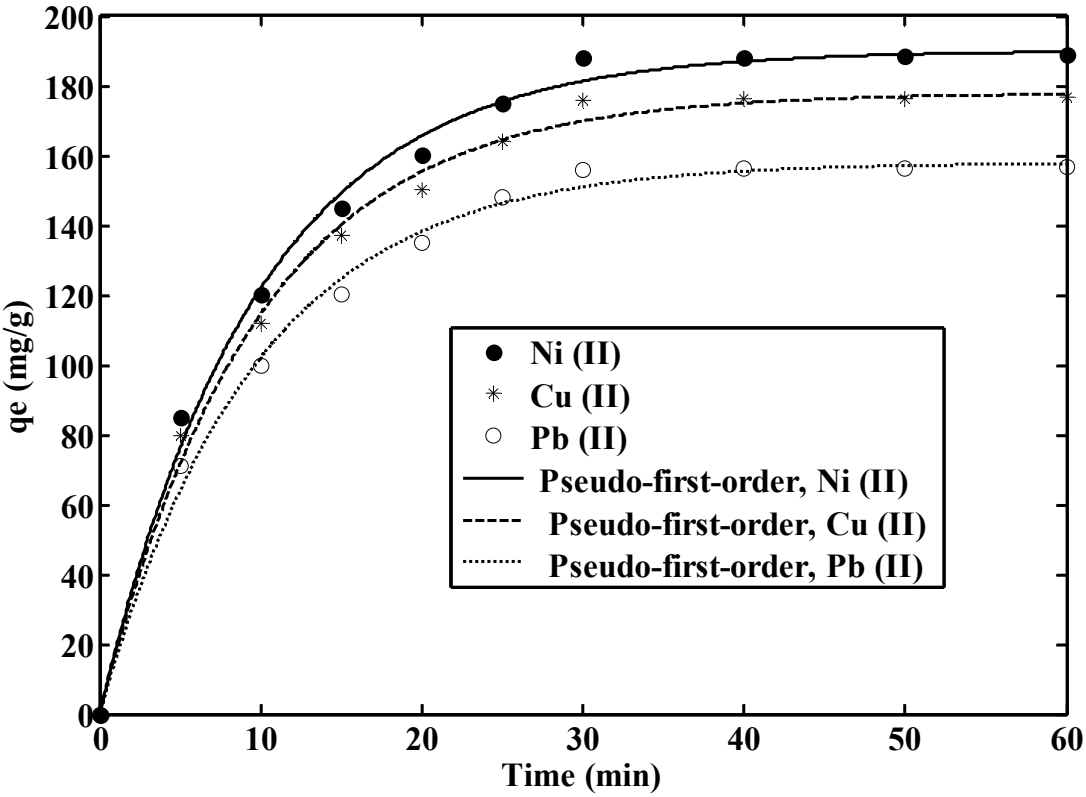

Fig.5

(a)

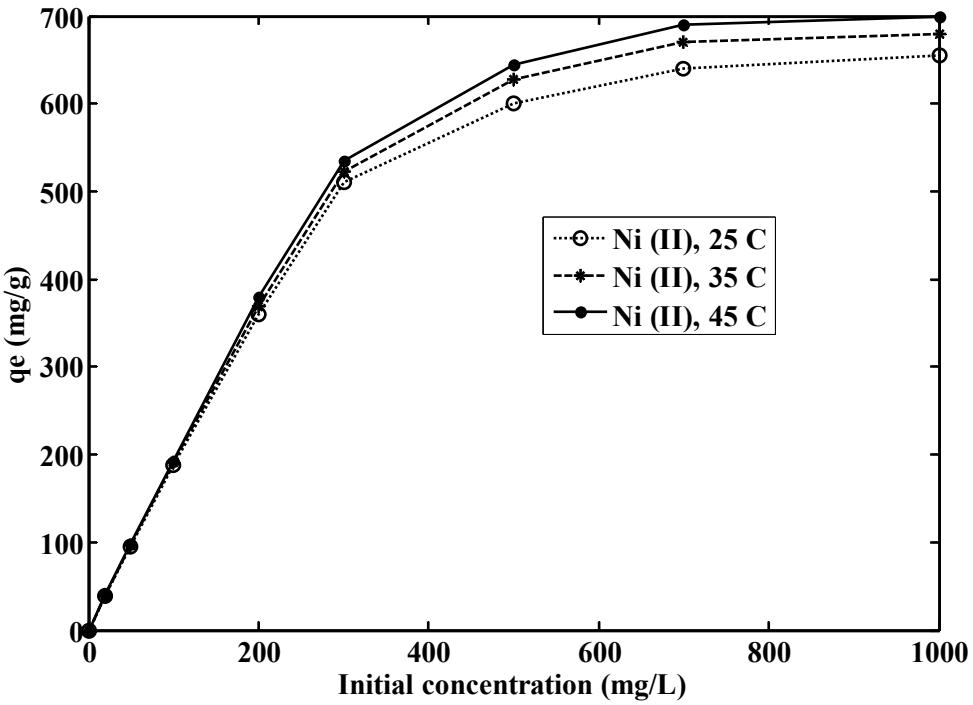

(b)

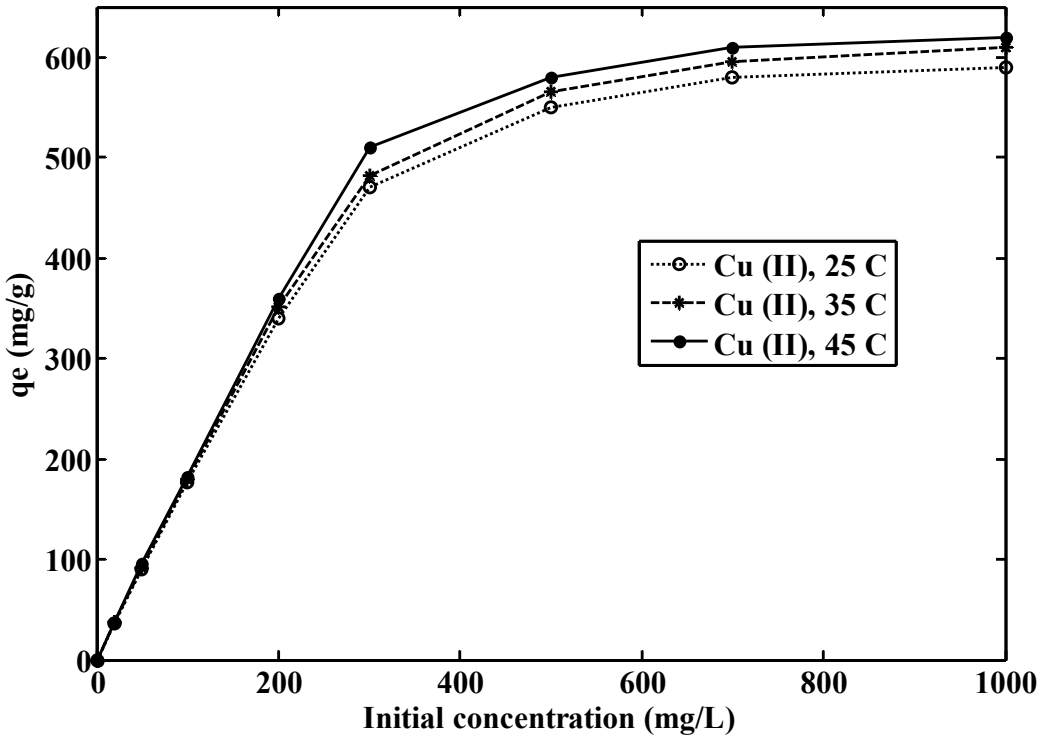

(c)

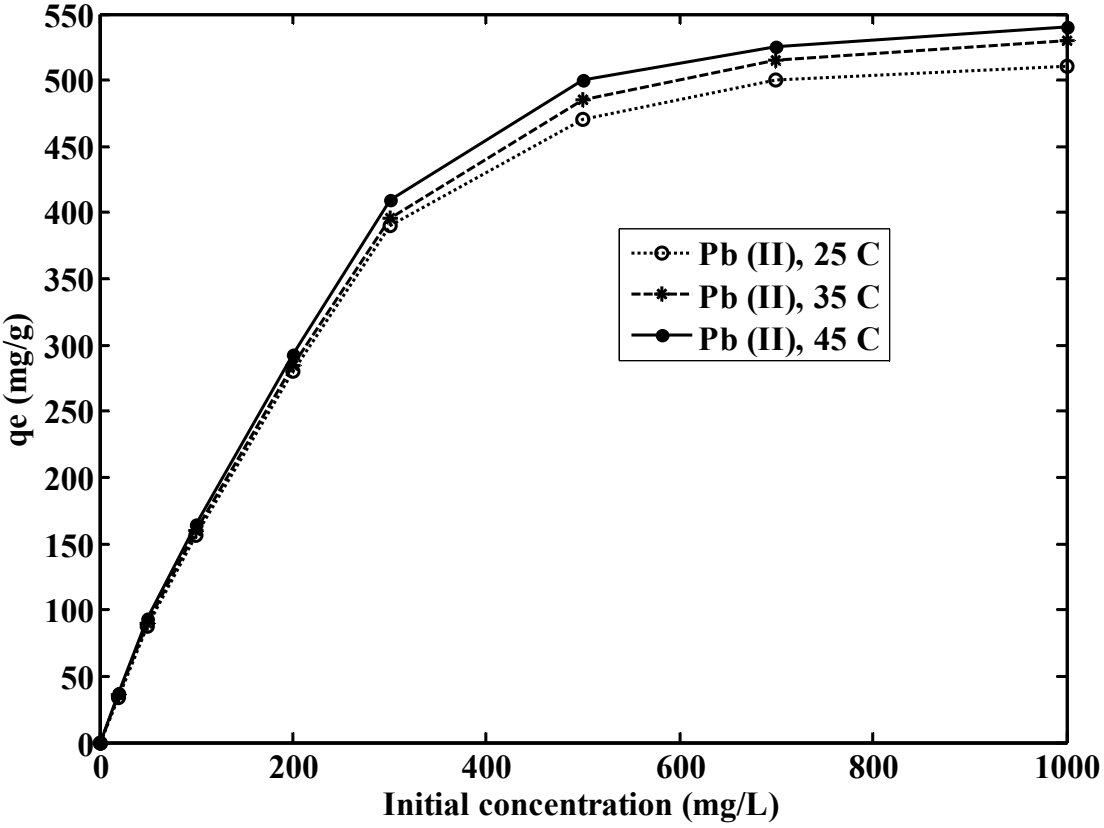

Fig.6

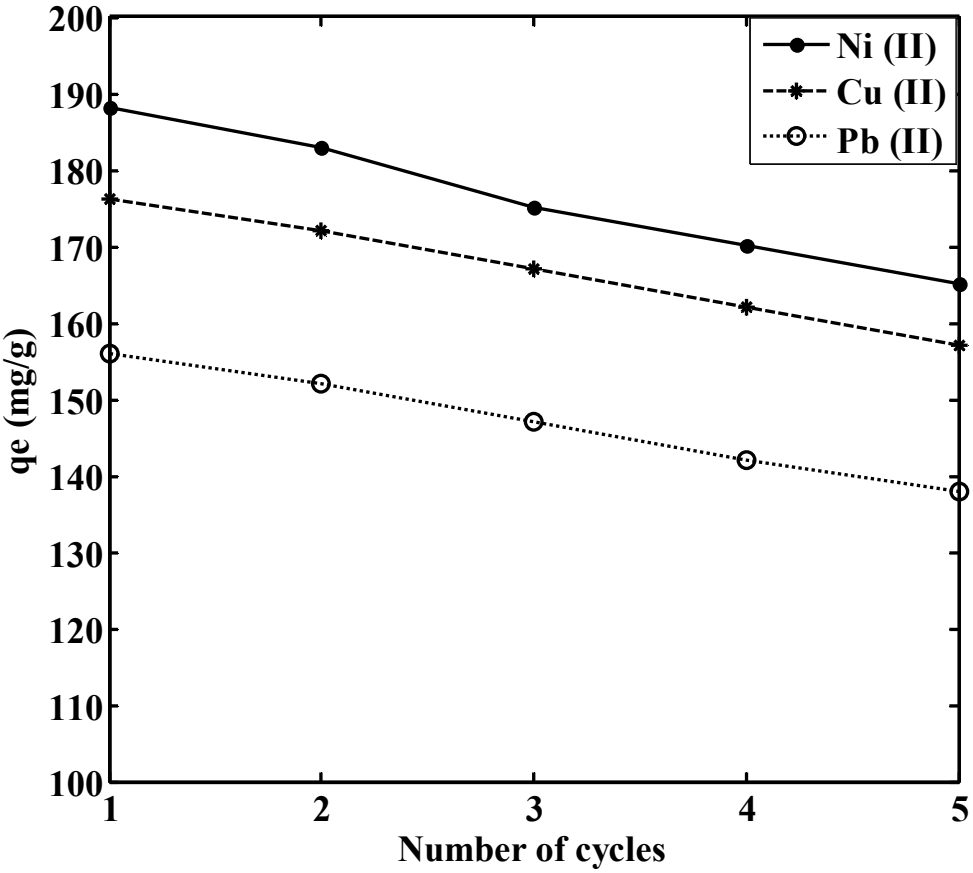

Fig.7

(a)

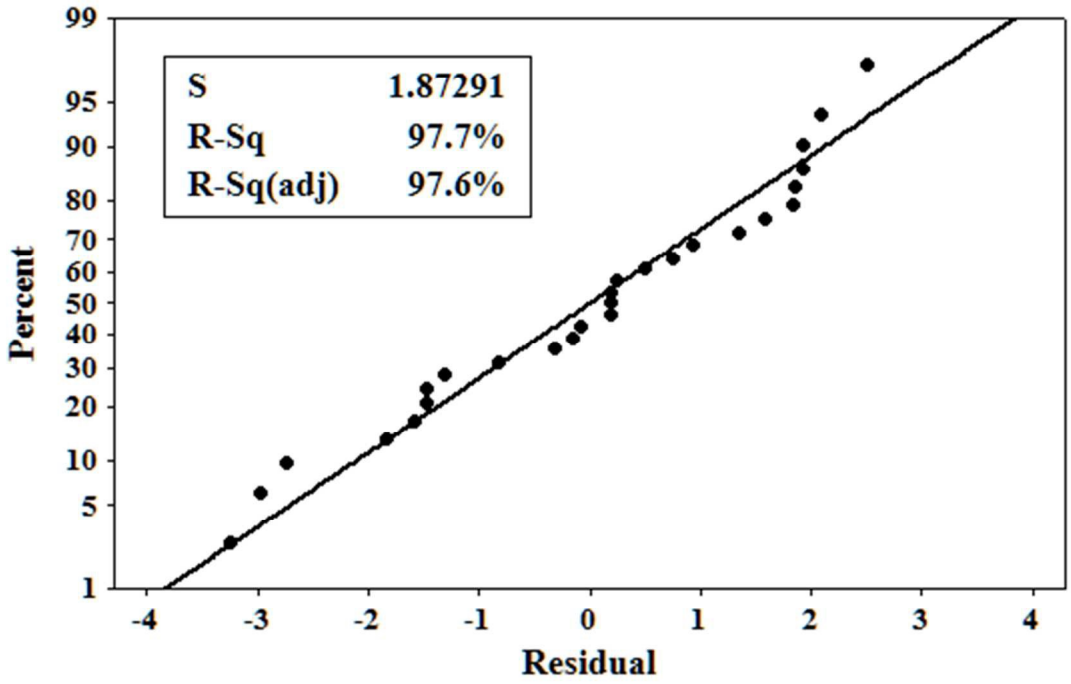

(b)

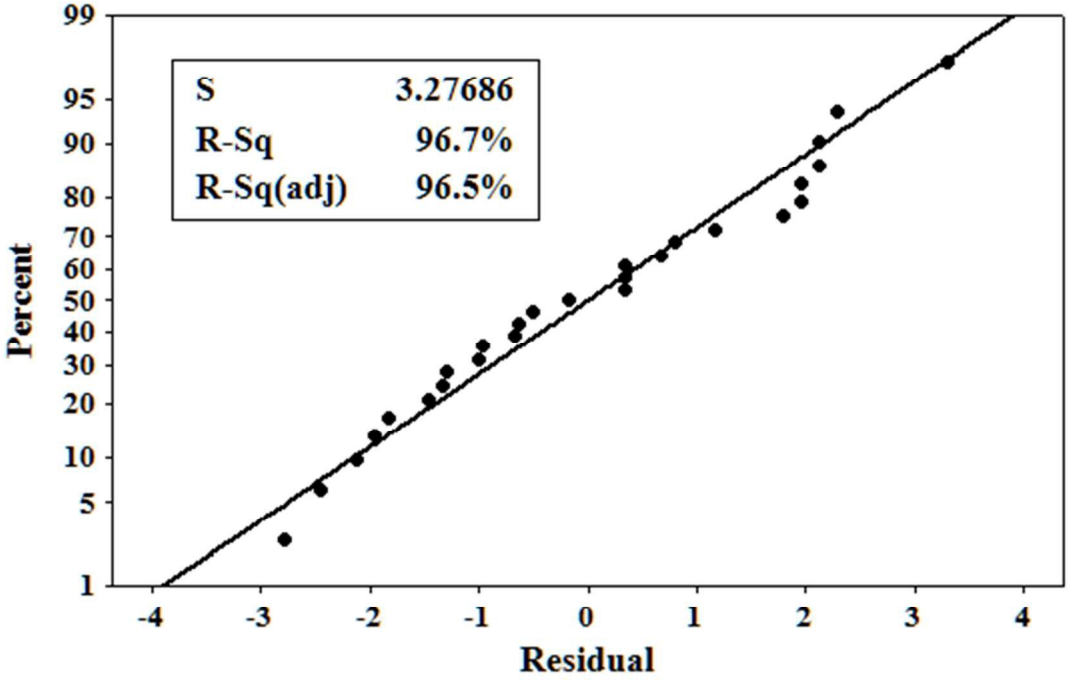

(c)

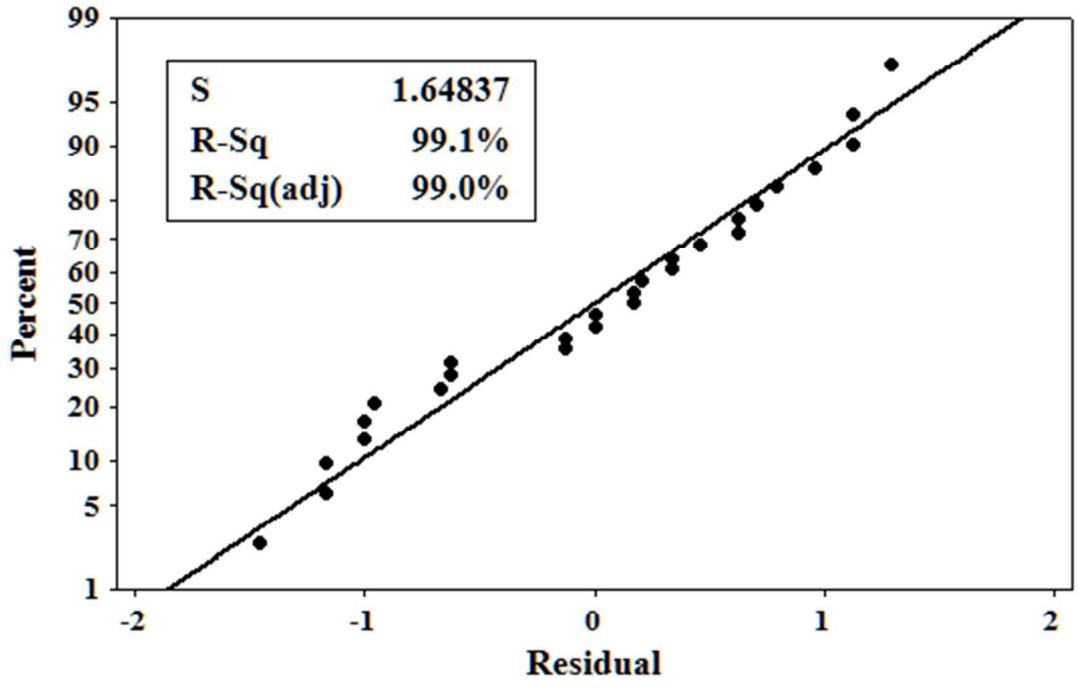

Fig.8

(a)

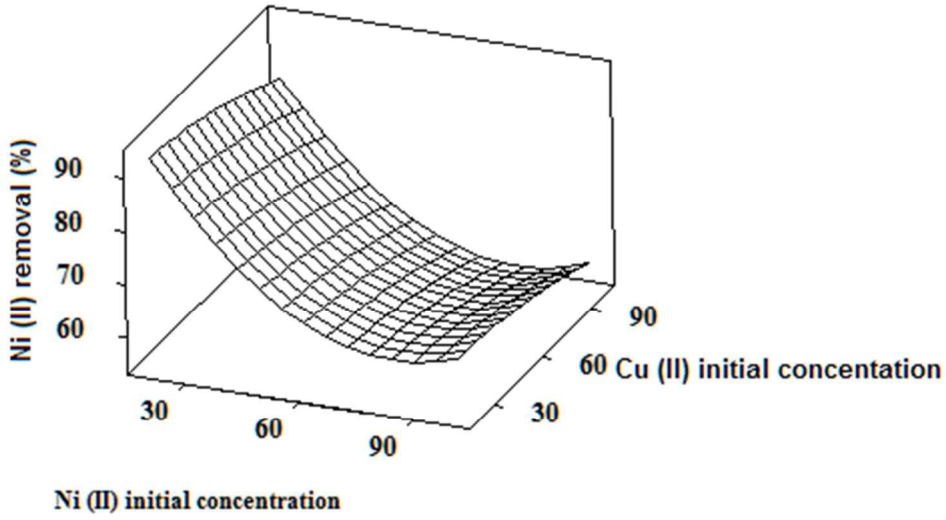

(b)

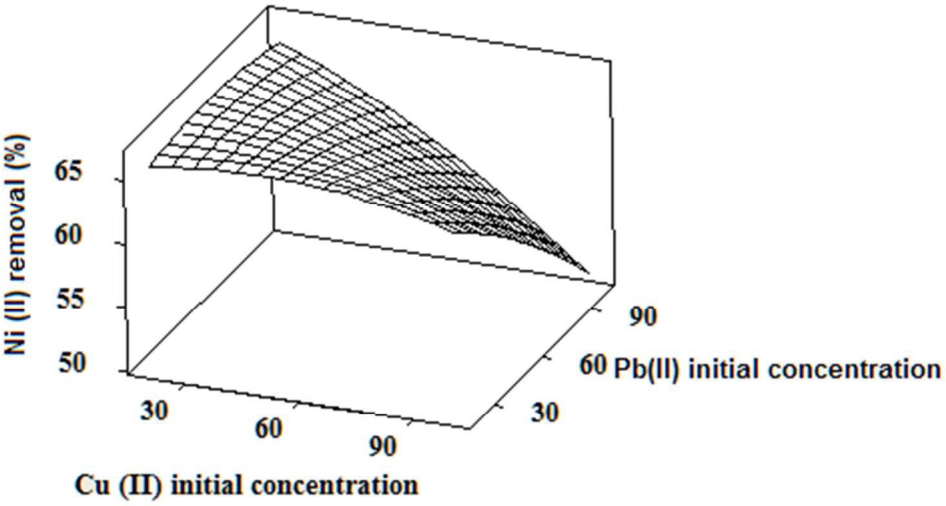

(c)

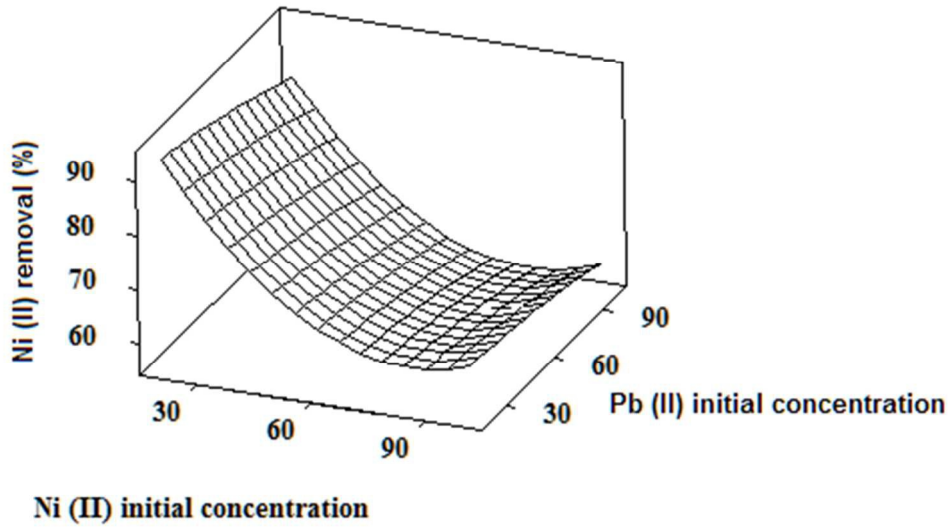

(d)

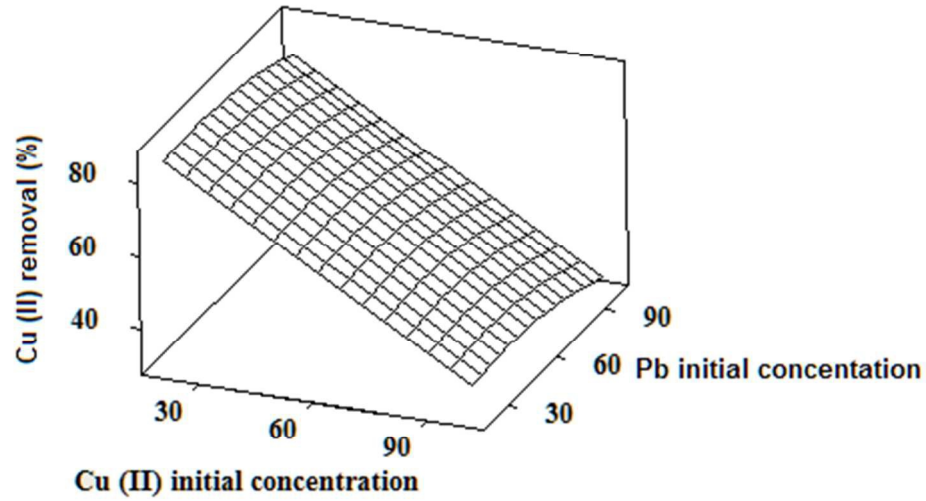

(e)

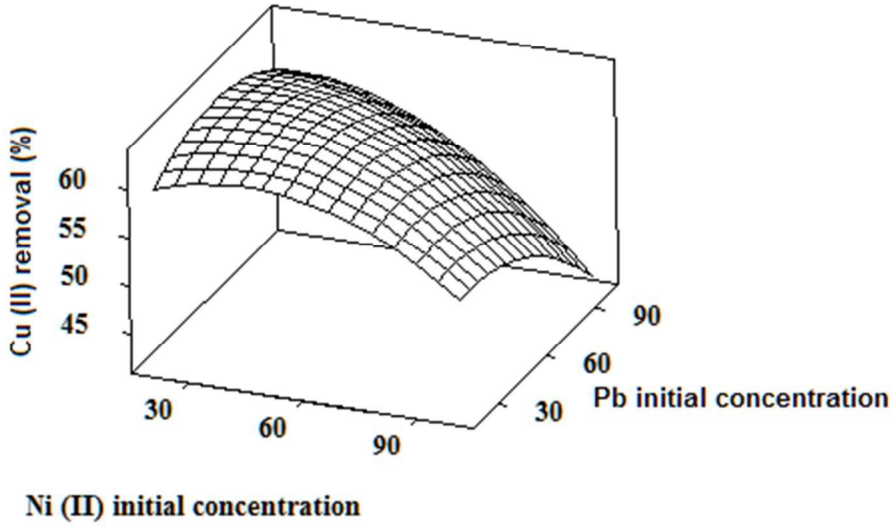

(f)

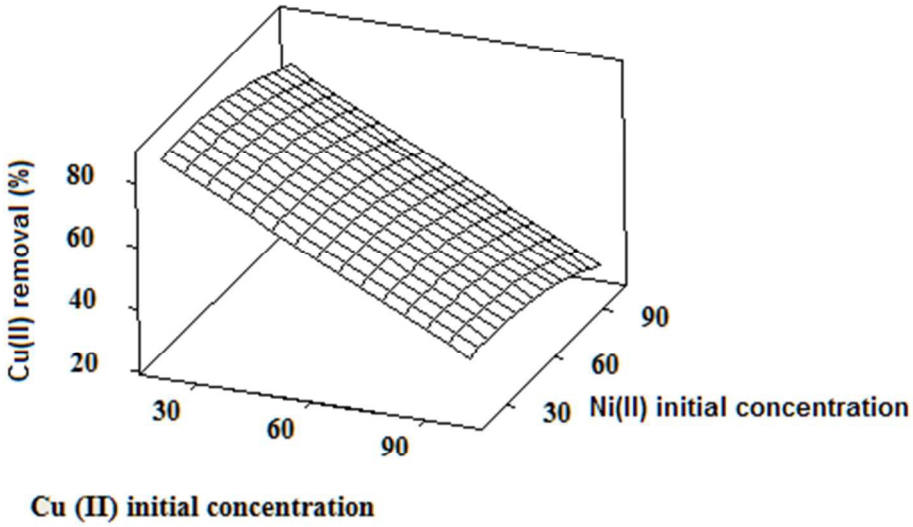

(g)

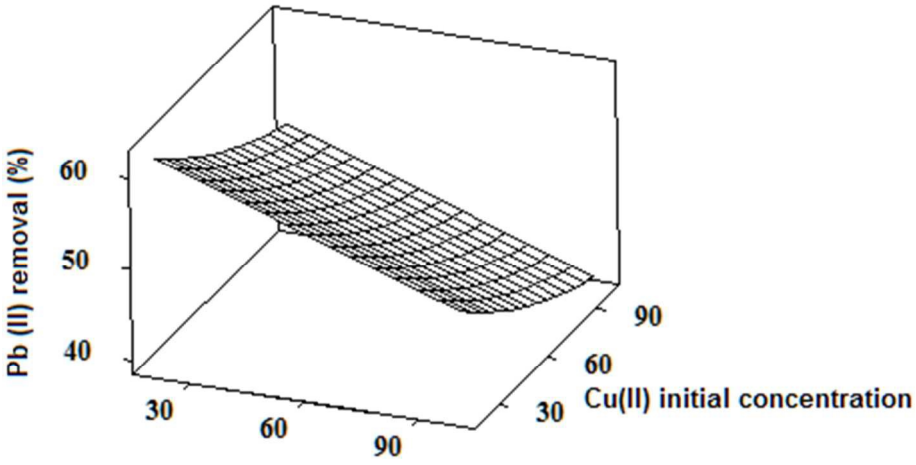

(h)

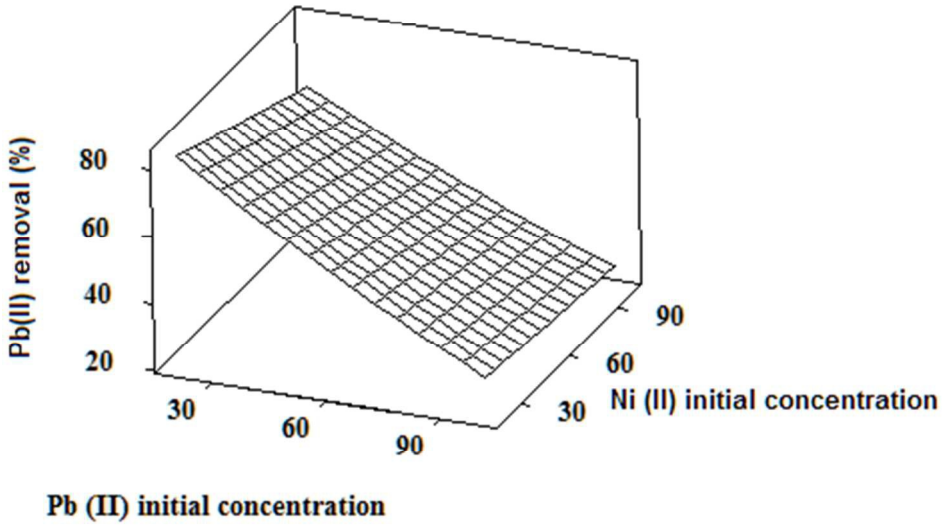

(i)

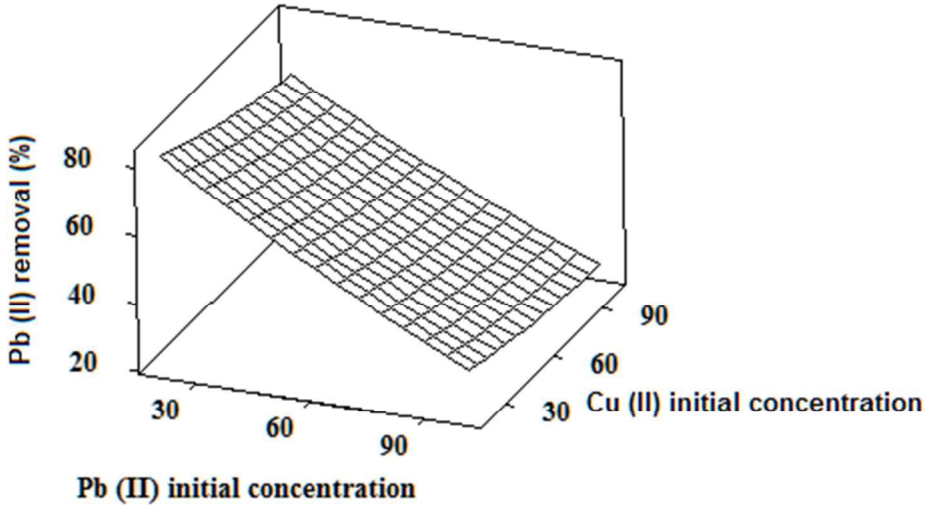

Fig.9

(a)

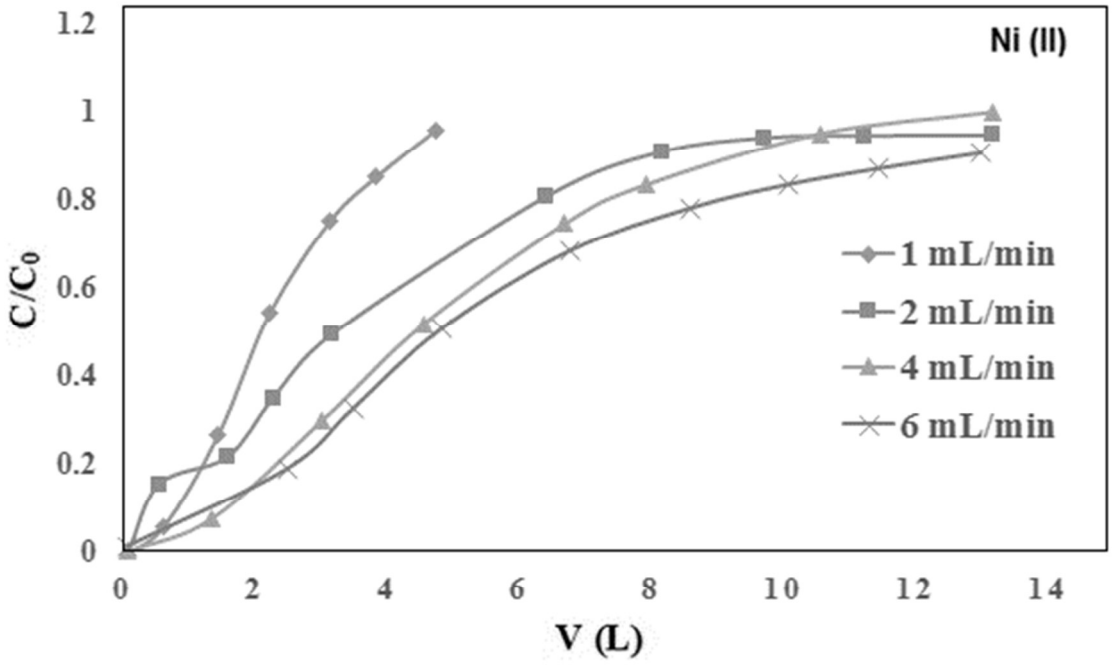

(b)

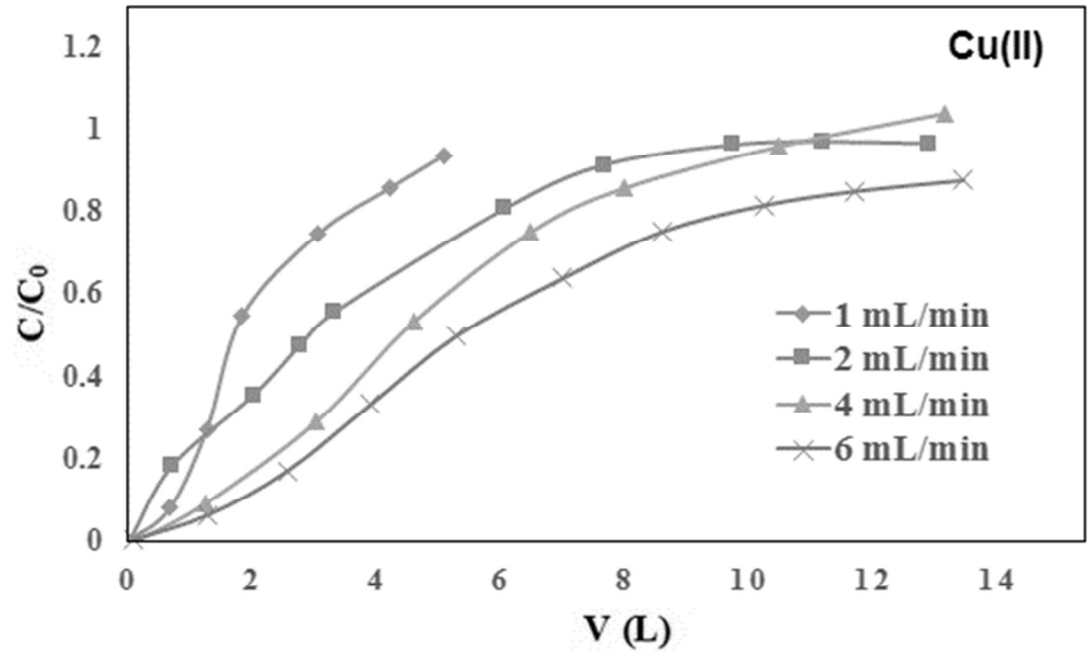

(c)

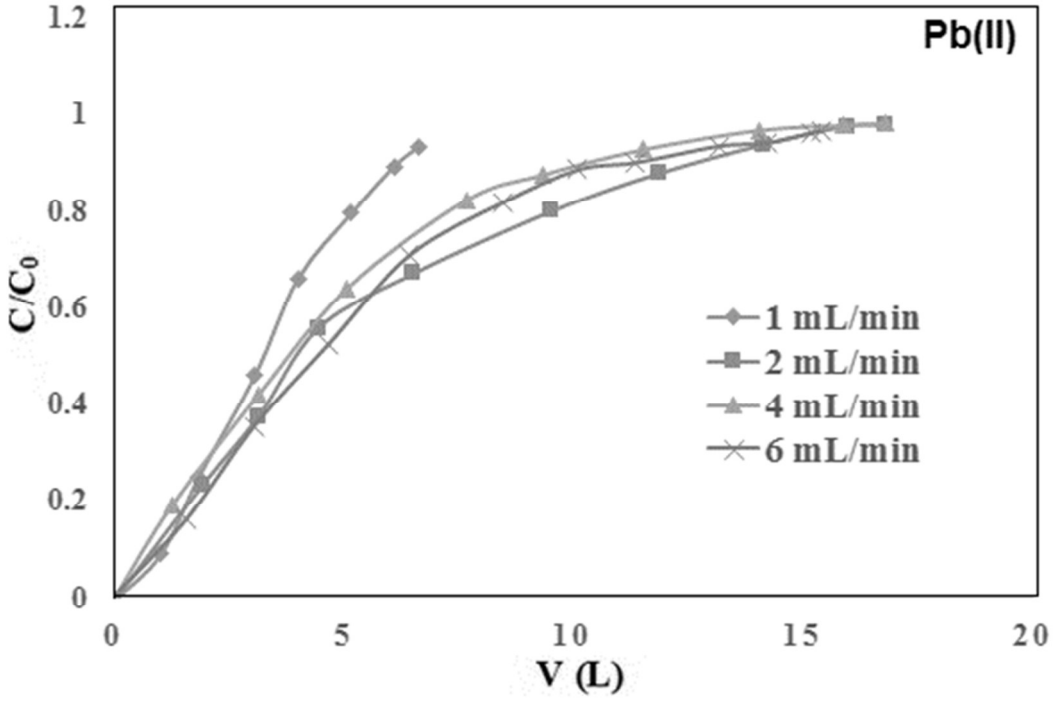

Fig.10

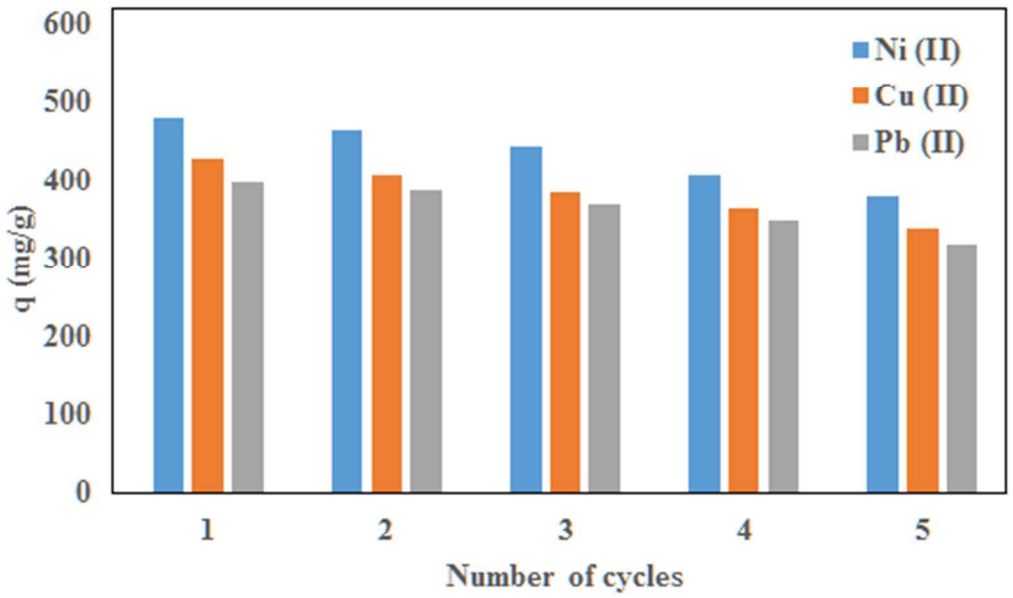

Graphical abstract

The homogeneous fibers with average diameters of 90 and 138 nm were formed for pure CS and CS/TEOS/APTES nanofibers.